

Photochemical & Photobiological Sciences

Accepted Manuscript

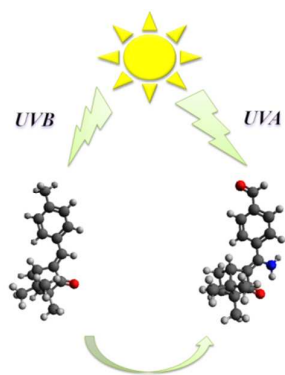


This is an *Accepted Manuscript*, which has been through the Royal Society of Chemistry peer review process and has been accepted for publication.

Accepted Manuscripts are published online shortly after acceptance, before technical editing, formatting and proof reading. Using this free service, authors can make their results available to the community, in citable form, before we publish the edited article. We will replace this *Accepted Manuscript* with the edited and formatted *Advance Article* as soon as it is available.

You can find more information about *Accepted Manuscripts* in the [Information for Authors](#).

Please note that technical editing may introduce minor changes to the text and/or graphics, which may alter content. The journal's standard [Terms & Conditions](#) and the [Ethical guidelines](#) still apply. In no event shall the Royal Society of Chemistry be held responsible for any errors or omissions in this *Accepted Manuscript* or any consequences arising from the use of any information it contains.



A theoretical methodology was used to characterize the UV absorption of the photo-stable UVB filter, 4-methylbenzylidene camphor. From this study resulted the design of two novel UVA filters.

Theoretical Study of the UV Absorption of 4-Methylbenzylidene Camphor: From the UVB to the UVA Region

Cite this: DOI: 10.1039/x0xx00000x

Received 00th January 2012,

Accepted 00th January 2012

DOI: 10.1039/x0xx00000x

www.rsc.org/

Luís Pinto da Silva,^a Paulo J.O. Ferreira,^a Margarida S. Miranda^a and Joaquim C.G. Esteves da Silva^{a*}

In this study, a theoretical approach was used to study the UV absorption of the UVB filter, 4-methylbenzylidene camphor. The main objective of this work was to design new UVA filters based on this rather photo-stable compound, so that photo-degradation on this UV region can be avoided without the use of other molecules. This objective was achieved by the simultaneous addition of two appropriate substituents, which led to red-shifts up to 0.69 eV while maintaining appreciable oscillator strengths. Also, useful structure-energy relationships were derived, which allow for the development of more UVA filters based on 4-methylbenzylidene camphor.

Introduction

The growing awareness of the harmful effects of the sun's UV radiation (280–400 nm) has led to an increase in the use of sunscreens. These commercial products are composed of organic or inorganic molecules known as UV filters.^{1–3} These compounds are able to absorb, reflect or scatter UV radiation (290–320 nm for UVB and 320–400 nm for UVA), thus minimizing/preventing health problems as sunburn, photo-aging and skin diseases (as skin cancer).^{4–8}

UV filters can be subdivided as inorganic, which reflect and scatter radiation, or organic, which absorb the UV radiation.^{1–3} While there are only two approved inorganic UV filters, the organic subsection is comprised by various classes of molecules: *para*-aminobenzoates, salicylates, cinnamates, benzophenones, dibenzoyl methanes, camphor derivatives and benzimidazoles.^{3,9,10} In general, organic UV filters possess one or more benzenic rings conjugated with electron donating and withdrawing groups in either *ortho* or *para* positions. This allows an efficient electronic delocalization, and renders the filters with a specific absorption wavelength.

After being exposed to solar radiation, the UV filters must be able to not only absorb the irradiation energy, but also to release this energy as heat before their decay or react with other molecules in their vicinity.^{11,12} If not, the UV-absorbing compound may undergo undesired photochemical reactions that result in photo-degradation and reduced effectiveness of the sunscreen.

Organic UV filters that provide protection in UVA region (320–400 nm) are quite rare. 4-*tert*-butyl-4'-methoxydibenzoyl-methane (commonly named Avobenzone, and here abbreviated to BMDMB) is one of such UVA filters, being the most widely used UVA filter in the world.^{13–16} In sunscreen formulations BMDMB exists predominantly in the enol form, which displays

high molar absorption coefficients with a maximum at 340–365 nm (depending on the solvent used).^{13–16} However, this UVA filter is known for its photo-instability.^{11,12,16–18} Upon absorption, BMDMB undergoes an enol → keto photo-tautomerism reaction and subsequent C–C bond breaking. While this process is not energetically favourable in the singlet bright state, intersystem crossing to the triplet state shifts the reaction to a more favourable potential energy surface of C–C bond breaking.^{16,19} Given this, several researchers have been trying to increase the stability of BMDMB upon irradiation. The most commonly used mechanism is to use another UV filter that can act as a triplet-triplet quencher.^{20–24}

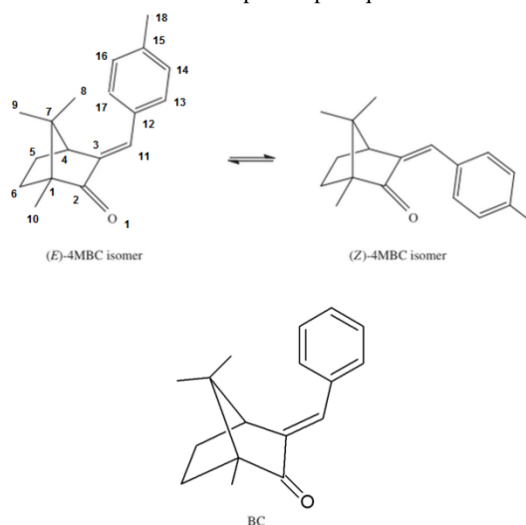


Figure 1. Schematic representation of the (*Z*) or (*E*)-isomers of 4-MBC, and of BC.

According to previous experimental works, 4-methylbenzylidene camphor (4-MBC, Figure 1) can be used as a stabilizer of BMDBM, as its first triplet state (T_1) is below that of BMDBM.^{25,26} 4-MBC is a very commonly used UV filter from the camphor derivative class of compounds. The absorption peak of this compound was found to be at 300 nm, and so, 4-MBC is used as a UVB filter.² This molecule is currently authorized in Europe and in Australia, and is being considered for use in the USA.²⁷ 4-MBC can exist as either a (*Z*) or (*E*)-isomer due to the exocyclic carbon-carbon (styrene) double bond (Figure 1).²⁸ Nevertheless, in the commercial formulation 4-MBC was shown to be present only as the (*E*)-isomer.²⁸ One of the advantages of 4-MBC over other UV filters is that it has been regarded as rather photostable, contrary to (for example) BMDBM.²⁹⁻³²

Here we present our theoretical study of the UV absorption of 4-MBC, its parent compound benzylidene camphor (BC, Figure 1), and a series of derivatives. With this study we intend to explore an alternative way of producing stable UVA filter molecules. Instead of trying to use combinations of UV filters, we intend to use an already stable compound (4-MBC) as starting point for the development of photostable UVA filters. Thus, our theoretical approach will be used to obtain structural-excitation energies relationships, and shift the absorption of 4-MBC from the UVB to the UVA region.

Computational Methods

All calculations were carried out using the Gaussian 09 program package.³³ The ground state (S_0) geometries of the studied UV filters were calculated at the PBE0/SV level of theory.^{34,35} Subsequent vibrational frequency calculations, at the same level of theory, were made to ensure that no imaginary frequencies were found for the S_0 structures.

The properties of the electronically singlet excited states (S_x) at the Franck-Condon state, were calculated with time-dependant (TD) density functional theory (DFT) single point calculations within the vertical approximation.^{36,37} The chosen density functional was CAM-B3LYP, while the basis set was SVP from Ahlrichs and co-workers.^{35,38}

The PBE0 functional was chosen due to good performance in geometry optimizations of organic compounds, as demonstrated by being the method of choice for obtaining geometric parameters in TD DFT benchmarks.³⁹⁻⁴¹ CAM-B3LYP was used for excited state single point calculations due to good results in local $n \rightarrow \pi^*$, $\pi \rightarrow \pi^*$, charge-transfer and Rydberg states.⁴² Moreover, we have already used this functional with good results in previous studies of UV filters.^{16,43}

Unless stated otherwise, all calculations were made *in vacuo*. When calculations were indeed performed in condensed phase, the solvent was modelled implicitly by using the conductor-like polarizable continuum model (CPCM).⁴⁴

The vibrationally resolved spectra within the harmonic approximation was calculated by using the Franck-Condon method implemented in Gaussian 09.³³ The reported spectra were simulated by using a convoluting Gaussian function presenting a half width at half maximum of 0.25 eV, in order to better compare with experimental results.²⁶ A maximal number of 50 overtones for each mode and 40 combinations on each pair of modes were included. The spectra were computed in implicit ethanol.

Results and Discussion

The *in vacuo* excited state properties of the (*E*)-isomers of 4-MBC and BC, at the Franck-Condon state, were calculated at the TD CAM-B3LYP/SVP level of theory, and the results are presented in Table 1. Both UV filters were placed on the UVB region of the spectrum. Also, the bright state for the molecules was the same: the S_2 state. BC presented an excitation energy of 4.51 eV, with an oscillator strength of 0.6962. The excitation of 4-MBC appears to be red-shifted (4.41 eV) and more efficient (0.7914) than that of BC, which should be attributed to the presence of a methyl substituent in the benzyl ring. Nevertheless, the Franck-Condon properties of 4-MBC and BC were found to be very similar, which indicates that the addition of a methyl group to the benzyl ring does not have a very significant effect on the optical properties of this kind of molecule.

Table 1. Excitation energies (E_{ex} , in eV), and oscillator strength (f) corresponding to the bright Franck-Condon state (S_x) of 4-MBC, BC, MBC₁₇, MBC₁₃ and MBC₁₁.

	S_x	E_{ex}	f
4-MBC	2	4.41	0.7914
BC	2	4.51	0.6962
MBC ₁₇	2	4.74	0.5059
MBC ₁₃	2	4.46	0.6085
MBC ₁₁	2	4.73	0.5389

The $S_0 \rightarrow S_2$ excitation of 4-MBC and BC is composed of a HOMO \rightarrow LUMO transition (Figure 2). Analysis of both orbitals clearly shows the $\pi \rightarrow \pi^*$ character of the transition. The HOMO is delocalized into the benzylidene moiety of 4-MBC and BC, and the oxygen atom of the camphor moiety. Upon excitation occurs a small electron density transfer, as now the LUMO is mainly localized in the styrene moiety.

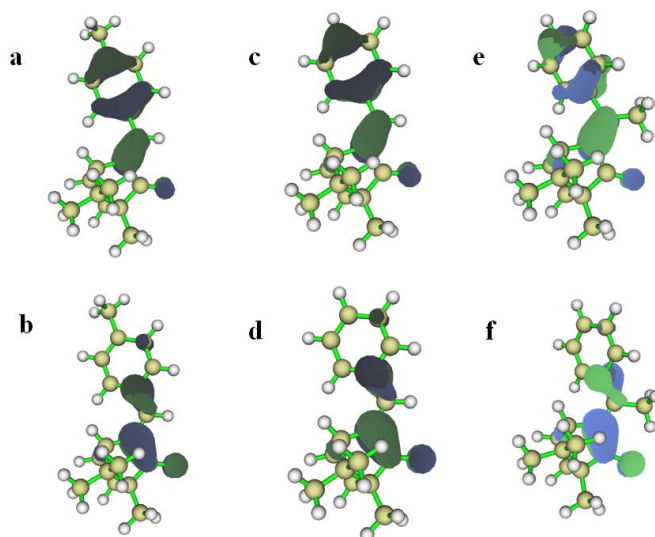


Figure 2. HOMO (a, c, and e) and LUMO (b, d, and f) orbitals of 4-MBC (a, b), BC (c, d) and MBC₁₁ (e, f).

This electron density localization upon excitation can be also seen, when the NBO atomic charges of 4-MBC and BC are calculated, both in the ground and Franck-Condon states (Table 2). The NBO atomic charges can be obtained by performing a natural bond analysis, which is an extension of a natural

population analysis (NPA). NPA involves constructing natural atomic orbitals on each centre, by dividing the electron density matrix into sub-blocks with appropriate symmetry. The charge is then partitioned in these orbitals. In the natural bond orbital analysis, the NPA charge is further partitioned into core and bonding orbitals, lone pairs and Rydberg states.

The polarity of these molecules increased slightly upon excitation, which means that the positive/negative charges of the molecules are more localized in the Franck-Condon state than in the ground state. This polarization can be explained by analysing the charge of the benzylidene, camphor and substituent moieties (Table 2). There are some differences between the charge density of 4-MBC and BC, which are expected to occur due to the methyl substituent of 4-MBC. In this latter molecule, the benzylidene moiety is positive in both states, although more positive in the Franck-Condon state. For the contrary, the camphor moiety is negative in both states. Thus, there is a negative charge transfer from the benzylidene to the camphor moiety, upon excitation. This is in line with our analysis of the HOMO \rightarrow LUMO transition (Figure 2). In the case of BC, both the benzylidene and camphor moieties are negative in the ground and Franck-Condon states. Nevertheless, one can also see a negative charge transfer from the benzylidene to the camphor moiety, upon excitation.

Table 2. NBO charges of the moieties of 4-MBC, BC and MBC₁₁, at the Franck-Condon and ground states. The ground state charges are presented between parentheses. The dipolar moment (in D) was also presented.

Moiety	4-MBC (R=CH ₃)	BC (R=H)	MBC ₁₁ (R=CH ₃)
Benzylidene	0.117 (0.074)	-0.084 (-0.125)	-0.117 (0.068)
Camphor	-0.171 (-0.116)	-0.139 (-0.105)	-0.178 (-0.125)
Substituent (R)	0.052 (0.042)	0.229 (0.228)	0.062 (0.057)
Dipolar moment	3.70	3.31	3.06

For gaining further insight into the Franck-Condon properties of these UV filters, we have used the Hirshfeld weighting function to decompose the contribution of a given atom. According to this function the composition (in percentage, %) of an atom A in an orbital i is $\int \varphi_i^2(r) w_A^{\text{Hirsh}}(r) dr \times 100\%$.⁴⁵ With the use of the Multiwfn code, we have resolved this function and obtain the contribution of each atom to the HOMO and LUMO orbitals of these filters.⁴⁶ The results are presented in Table 3 for atoms that presented contributions equal or higher than 5.0%.

Table 3. Atomic contribution (in %) for the HOMO and LUMO orbitals of 4-MBC, BC and MBC₁₁. Only atoms with contributions equal or higher than 5.0 % were considered. The contributions for the LUMO orbital are present between parentheses.

	4-MBC	BC	MBC ₁₁
O ₁	6.0 (13.3)	6.7 (13.7)	6.3 (16.0)
C ₂	(10.4)	(10.6)	(12.9)
C ₃	17.2 (25.3)	18.6 (26.5)	19.9 (26.7)
C ₁₁	10.9 (7.7)	12.8 (7.3)	13.9 (6.5)
C ₁₂	12.9 (16.7)	12.1 (16.3)	10.7 (13.2)
C ₁₅	13.0	12.9	10.9
C ₁₇	6.7	7.0	6.0

In terms of atomic contributions for both the HOMO and LUMO orbitals, in percentage, there is little difference between 4-MBC and BC. The atoms that presented contributions equal or higher than 5.0% for the HOMO, are C₁₅, C₁₇, C₁₂, C₁₃, C₁₁, C₃ and O₁. C₃ is clearly the atom with a higher contribution. Nevertheless, C₁₅, C₁₂ and C₁₁ also present significant contributions. C₁₇, C₁₃ and O₁ present lower contributions. In the case of the LUMO, there are fewer atoms with contributions equal or higher than 5.0%: C₁₂, C₁₁, C₃, C₂ and O₁. The major contributor to the LUMO is C₃, followed by O₁ and C₁₂. Thus, our analysis indicates that C₁₂, C₁₁, C₃ and O₁ contribute for both HOMO and LUMO. Moreover, C₃ is the major contributor for both orbitals. C₁₅, C₁₇, and C₁₃ contribute only for the HOMO, while C₂ only contributes for the LUMO.

While these results give us insight regarding the optical transitions of these filters, they do not explain why the excitation of 4-MBC is more red-shifted than that of BC. In order to explain this red-shift, we have calculated the atomic partial charges of the atoms involved in the HOMO orbital, in the ground state, and the charges of the atoms involved in the LUMO orbital, corresponding to the Franck-Condon state. The results are present in Table 4. The sum of the charges of the atoms involved in the HOMO gives a significant negative value (-1.328 for 4-MBC and -1.526 for BC). This lower negative charge for 4-MBC is due to significant decrease in the negative charge of C₁₅, when comparing with BC. The sum of the charges of the atoms involved in the LUMO also gives a negative value for both molecules. However, the obtained values are lower than that found for the HOMO. There is once again a difference in charge between 4-MBC and BC. The latter UV filter has a lower negative charge than the former. This is due to an increase of the negative charge of the C₁₂ atom. Thus, the addition of a methyl group to the benzyl ring changed the charge of two atoms (C₁₅ and C₁₂), which have significant contributions for the HOMO and LUMO, respectively (Tables 3 and 4).

Table 4. NBO charges of the atoms that contribute for the HOMO and LUMO orbitals of 4-MBC, BC and MBC₁₁. Charges related to HOMO correspond to ground state NBO charges, while charges related to the LUMO correspond to Franck-Condon NBO charges. Only atoms with contributions equal or higher than 5.0 % were considered. The Franck-Condon NBO charges are present between parentheses.

	4-MBC	BC	MBC ₁₁
O ₁	-0.573 (-0.606)	-0.570 (-0.602)	-0.580 (-0.624)
C ₂	(0.492)	(0.490)	(0.457)
C ₃	-0.129 (-0.038)	-0.124 (-0.026)	-0.142 (-0.012)
C ₁₁	-0.138 (-0.221)	-0.141 (-0.206)	0.065 (0.003)
C ₁₂	-0.089 (-0.190)	-0.080 (-0.027)	-0.065 (-0.019)
C ₁₅	-0.025	-0.217	-0.221
C ₁₇	-0.190	-0.200	-0.209
Total HOMO charge	-1.328	-1.526	-1.358
Total LUMO charge	-0.563	-0.371	-0.195

The obtained results have then indicated that the excitation energy of 4-MBC is red-shifted when in comparison with BC, as the addition of the methyl group to the benzyl group affected the charge density of the HOMO and the LUMO orbitals. However, our results do not allow us to conclude if this red-shift is the result of decreasing the negative charge of the HOMO, of increasing the negative charge of the LUMO, or of the combination of both processes. In order to gain further insight, we created three new methylated BC derivatives: one methylated at C₁₇ (MBC₁₇), other methylated at C₁₃ (MBC₁₃), and another methylated at C₁₁ (MBC₁₁). C₁₃ and C₁₇ atoms are atomic contributors of the HOMO orbital for 4-MBC and BC, while C₁₁ contributes for both HOMO and LUMO orbitals.

The computed excitation energies and oscillator strengths of these new BC derivatives are present in Table 1. MBC₁₃ is slightly red-shifted in regard to BC, but slightly blue-shifted when comparing with 4-MBC. MBC₁₇ and MBC₁₁ present very similar excitation energies, which are significantly blue-shifted when in comparison with BC (~0.22 eV) and 4-MBC (~0.32 eV). Once again the bright transition was found to be the S₀ → S₂ one. For MBC₁₁ this S₀ → S₂ excitation is composed by a HOMO → LUMO orbital transition (Figures 2.e and 2.f). The HOMO appears to be delocalized upon the π system of MBC₁₁, while the LUMO is more localized upon the styrene moiety of this molecule. The analysis of the HOMO and LUMO also allows characterizing this excitation as of the π → π*. This is in line with what was found for BC and 4-MBC in this study. However, this is not the case of MBC₁₃ and MBC₁₇. Indeed, the main orbital transition is once again the HOMO → LUMO one (93.4% for MBC₁₃, and 86.6% for MBC₁₇). However, this is now not the only one, as the S₀ → S₂ excitation is composed also by a HOMO(-1) → LUMO transition (3.1% for MBC₁₃, and 9.5% for MBC₁₇). Moreover, while the HOMO → LUMO transition has π → π* character, the HOMO(-1) → LUMO transition appears to be of the n → π* type (Figure S1). As the excitation of MBC₁₃ and MBC₁₇ present a significant difference in nature in regard to that of 4-MBC, thereby impairing comparative studies, these two molecules were not further analyzed. Nevertheless, our present calculations indicate that the methylation of the C₁₃ and C₁₇ atoms has no particular advantage, when in comparison with the methylation present in 4-MBC.

The NBO partial atomic charges of MBC₁₁, at the ground and Franck-Condon states, can be found on Table 2. The methylation of C₁₁ has a similar effect to that exerted by the methylation present in 4-MBC. However, the charge difference between these two moieties is larger for MBC₁₁ than for 4-MBC. Upon excitation, there is a negative charge transfer from the benzylidene to the camphor moiety, which explains the increase in the dipolar moment. This is in line with the NBO charge analysis made for 4-MBC and BC.

The contribution of each atom of MBC₁₁ to the HOMO and LUMO was also calculated, by using the Hirshfeld weighting function present in Multiwfn code and the results can be seen in Table 3. The atoms that contribute for the HOMO and LUMO of MBC₁₁ are the same that contribute for the same orbitals of 4-MBC and BC. There is also little difference in the percentage of each contribution. Thus, our results indicate that the significant blue-shift of MBC₁₁ is not due to any change in the atomic contribution profile to the HOMO and LUMO.

Once again, we have calculated the atomic partial charges of MBC₁₁ for the atoms involved in the HOMO orbital, in the ground state, and for the atoms involved in the LUMO orbital,

corresponding to the Franck-Condon state. The results are present in Table 4.

No relationship appears to exist between the charge of the HOMO orbital and the excitation energies of these compounds. The least negative HOMO belongs to 4-MBC (with the lowest excitation energy), followed by MBC₁₁ (with the highest excitation energy) and then by BC (with the middle excitation energy). This decreased HOMO negative charge of MBC₁₁, in comparison with BC, is due to a different atomic charge of the C₁₁ atom. The methylation of this atom led to change from a negative charge, in BC, to a positive partial charge in MBC₁₁. The sum of the atomic charges for the LUMO also is affected by the degree and location of methylation substitution. The methylation of C₁₁ decreased significantly the negative charge of the LUMO, when comparing with both BC and 4-MBC. This effect was also due to atom C₁₁. Its methylation led from a shift from a charge of -0.206 (in BC) to 0.003 (in MBC₁₁). In a matter of fact, we have found that there is a correlation between the excitation energy of these filters and the sum of the LUMO charge. More specifically, it appears that the excitation energy decreases with increasing negative LUMO charge. Moreover, we have found that methylation of C₁₅ increases this negative charge, while methylation of C₁₁ decreases it. In this system, the methyl substituent acts as electron-withdrawing for the benzylidene moiety (Table 2). Thus, our results indicate that addition of electron-withdrawing substituents to C₁₅, and electron-donating ones to C₁₁, should decrease the excitation energies of the BC family of compounds.

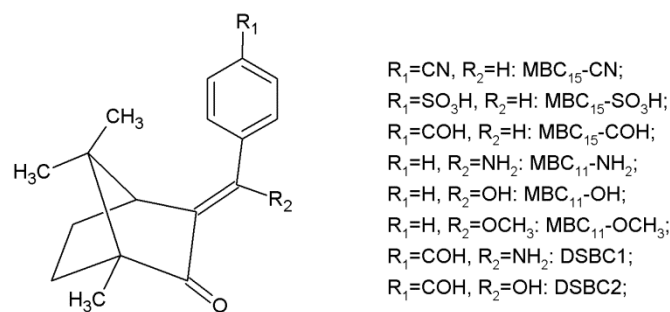


Figure 3. Schematic representation of the newly designed BC derivatives.

In order to confirm this prediction, we have studied six new BC derivatives (Figure 3). Three were the result of the addition of electron-withdrawing substituents to C₁₅: MBC₁₅-CN (addition of a cyanide group), MBC₁₅-SO₃H (addition of a sulfonic acid group), and MBC₁₅-COH (addition of an aldehyde group). The other derivatives resulted from the addition of electron-donating substituents to C₁₁: MBC₁₁-NH₂ (addition of an amine group), MBC₁₁-OH (addition of a hydroxyl group), and MBC₁₁-OCH₃ (addition of a methoxy group).

Table 5. Excitation energies (in eV) of 4-MBC, BC and several single substituted derivatives, in water, ethanol and *in vacuo*. The oscillator strengths are presented between parentheses.

	<i>In vacuo</i>	Ethanol	Water
MBC ₁₁ -NH ₂	4.16 (0.3647)	3.99 (0.5543)	3.98 (0.5619)
MBC ₁₅ -COH	4.23 (0.8925)	3.94 (1.1812)	3.93 (1.1906)
MBC ₁₁ -OH	4.25 (0.5092)	4.01 (0.7500)	4.01 (0.7563)
MBC ₁₅ -CN	4.33 (0.9014)	4.05 (1.2063)	4.04 (1.2168)
MBC ₁₁ -OCH ₃	4.37 (0.4663)	4.15 (0.7085)	4.14 (0.7177)
4-MBC	4.41 (0.7914)	4.11 (1.0604)	4.10 (1.0694)
MBC ₁₅ -SO ₃ H	4.44 (0.8601)	4.18 (1.1257)	4.17 (1.1348)
BC	4.51 (0.6962)	4.21 (0.9696)	4.19 (0.9793)
MBC ₁₁	4.73 (0.5389)	4.47 (0.8007)	4.46 (0.8107)

The computed excitation energies and oscillator strengths of these new BC derivatives are present in Table 5. The results were also presented for 4-MBC, BC and MBC₁₁. Besides the *in vacuo* results, the Franck-Condon state of all these molecules were computed in the condensed phase. The solvent was taken into account implicitly, by performing solvated single point calculations on the *in vacuo* geometries. The chosen solvents were ethanol and water.

The first thing to note is that the solvated excitation energies calculated for 4-MBC are well in line with experiment, with only a difference of 0.02/0.03 eV.² This finding supports the use of the presented theoretical methods. Secondly, these results indicate that our predictions came true, as all new derivatives were red-shifted when in comparison with BC. Also, all but two derivatives (MBC₁₁-OCH₃ and MBC₁₅-SO₃H) presented excitation energies lower than 4-MBC. Moreover, these shifts were particularly significant, with decreases in energy up to 0.25 and 0.34 eV (for 4-MBC and BC, respectively). MBC₁₁-NH₂ led to the larger red-shift *in vacuo*, followed by MBC₁₁-OH and MBC₁₅-COH. In condensed phase, MBC₁₅-COH became the most red-shifted molecule, now followed by MBC₁₁-NH₂ and MBC₁₁-OH. The other substitutions only caused more modest energy decreases, when comparing with 4-MBC. It should be noted that the addition of implicit solvent red-shifted considerably the excitation energies of all BC derivatives. Nevertheless, only a negligible difference was found for the results for different solvents.

Interestingly, it appears that both locations of substitution (atom C₁₅ or C₁₁) can cause similar extents of red-shift. Nevertheless, one can see that the oscillator strength is higher than the one present by 4-MBC/BC if the substitution is made on atom C₁₅. If the substitution is made on atom C₁₁, the oscillator strength is shown to be smaller than the one presented by 4-MBC/BC. Thus, our results indicate that the preferential localization of substitution should be atom C₁₅, in order to obtain both a red-shifted excitation and increased oscillator strength. Nevertheless, one should not be oblivious to the fact that the addition of electron-donating groups to C₁₁ decreased more

significantly the excitation energy of BC, than the addition of electron-withdrawing groups to C₁₅.

It should be noted that the conclusions here presented do not exclude the possibility of obtaining useful excitation energies and/or oscillator strength, when adding substituents to other carbon atoms than C₁₁ and C₁₅. We have focused on substitution of C₁₁ and C₁₅ as we wanted to present useful UV absorption-structure relationships, and addition of substituents to other carbon atoms (C₁₃ and C₁₇) altered the excitation transitions in a way that could impair further comparative studies (as already referred). Nevertheless, we do believe that other carbon atoms than the ones present in the benzylidene moiety do not present a great potential to alter the absorption profile, as they are not involved in the HOMO → LUMO transition (Figure 2).

Table 6. Excitation energies (E_{ex} , in eV), and oscillator strength (f) corresponding to the bright Franck-Condon state (S_x) of DSBC1 and DSBC2. The results were obtained *in vacuo*, and in implicit ethanol and water.

	DSBC1		DSBC2	
	E_{ex}	f	E_{ex}	f
<i>In vacuo</i>	3.72	0.2938	3.99	0.5915
Ethanol	3.61	0.4994	3.76	0.8566
Water	3.60	0.5075	3.75	0.8534

Having analyzed the effect of substituents addition to C₁₁ and C₁₅, the logical next step is to analyze the effect of adding new moieties to both atoms at the same time. If the red-shift obtained from modifications of both atoms could be additive, it should be possible to obtain a new UVA BC derivative. To this end, we have created a new BC derivative: doubly substituted BC 1 (DSBC1, Figure 3). This derivative resulted from the addition of an aldehyde group to C₁₅, and an amine group to C₁₁. These groups were chosen as they were the ones to provide the greater red-shifts. The BC derivative DSBC2 (Figure 3) was also created. This molecule maintained the aldehyde group, but the amine one was changed for a hydroxyl group. This difference arises from the fact that the amine group decreased very significantly the oscillator strength of MBC₁₁-NH₂, when in comparison with BC (Table 5). This could be prejudicial to the effectiveness of this molecule as a UV filter. The addition of a hydroxyl group to C₁₁ also decreased the oscillator strength, but to a lesser extent. Moreover, the addition of a hydroxyl group was also responsible for a significant red-shift. The computed excitation energies and oscillator strengths of these new BC derivatives are present in Table 6. These properties were calculated *in vacuo*, and also in implicit ethanol, and water.

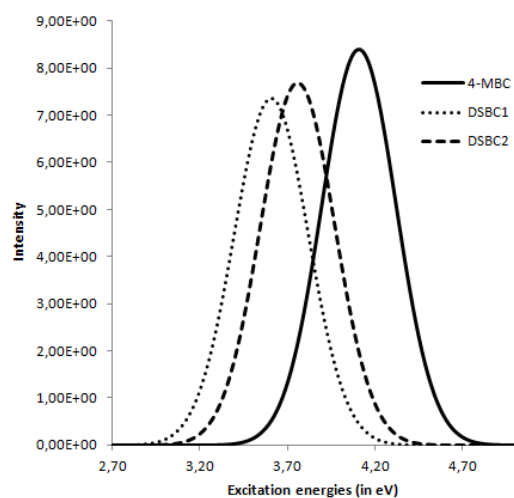


Figure 4. Calculated excitation spectra, in ethanol, of 4-MBC, DSBC1 and DSBC2.

The results obtained for these new derivatives were very interesting and promising. The addition of both aldehyde/amino and aldehyde/hydroxyl groups to BC lead to a shift in the absorption from the UVB to the UVA region. This is translated in red-shifts of 0.49-0.69/0.35-0.42 eV for DSBC1 and DSCB2, respectively, when comparing with 4-MBC. For DSBC1 this shift occurred in the gas and in condensed phases, while for DSBC2 the absorption was still in the UVB region in the gas phase. Nevertheless, as the practical applications of the UV filters occur in condensed phase, even DSBC2 appears to be a promising UVA filter.

It should be noted that the red-shift caused by these double substitutions is higher than the sum of the corresponding single substitutions. For example, when only an amino group was added to BC, the red-shift was of 0.12-0.25 eV when in comparison with 4-MBC. The red-shift in absorption was of 0.17 eV when the substituent was the aldehyde group. The sum of these red-shifts leads to an energy decrease of 0.28-0.42 eV. However, in the case of DSBC1 (when these two groups are added at the same time to BC) the red-shift is 0.21-0.27 eV higher than the simple addition of these red-shifts. The situation is similar for DSBC2.

The drawback of these new structures is associated with their calculated oscillator strength. As expected by us, the oscillator strength of DSBC1 is lower than the one presented by DSCB2. However, both compounds present oscillator strengths lower than the ones presented by 4-MBC (Tables 5 and 6). This indicates that the next step in the study of BC derivatives is to understand the mechanism behind the modulation of the oscillator strength. Nevertheless, in our opinion the computed oscillator strengths for DSBC1/DSBC2 are still appreciably high, and do not invalidate these compounds as potential UVA filters.

It should be noted that the optical properties of a given molecule do not depend only of its excitation energy and oscillator strength, but also on the shape of the absorption band (including its vibronic structure). Given this, we proceeded to calculate the vibrationally resolved electronically spectrum of DSBC1, DSBC2 and 4-MBC (Figure 4).⁴⁷ The spectra were calculated in the basis of the so called linear coupling model (LCM, also known as vertical gradient model).^{48,49} This model assumes that the normal modes of the initial and final states are only displaced, and so, it is only required the computation of

the gradient of the final state PES at the geometry of the initial state. This assumption is based on the observation that the transitions with higher intensity are vertical. Therefore, it is more suitable to analyze the region of the spectral maximum and the broad features of the spectrum, if the PES of the final state is described about the geometry of the initial state.⁴⁷ The spectra were obtained in ethanol, in order to better compare with a recent experimentally obtained absorption spectrum of 4-MBC. This was obtained by calculating the initial state geometry in the gas phase, as well as the Hessian, and the energies and corresponding gradients of both the initial and final states in implicit ethanol.

The experimental absorption spectrum of 4-MBC, in ethanol, is characterized by an intense and broad band in the UVB region.²⁶ This feature of the spectrum is indeed captured by our calculated vibrationally resolved spectrum of 4-MBC, thus supporting the use of the current methodology. Interestingly, this feature is conserved in both DSBC1 and DSBC2. In fact, the spectra of all three molecules are almost identical, with exception of their excitation maximum and peak height. Therefore, the present data indicate that addition of novel substituents to C₁₁ and C₁₅ does not alter the shape of the absorption of the filter, but only the excitation maximum and the peak height.

Conclusions

In this study, we have used a theoretical methodology to characterize the UV absorption of 4-MBC and derivatives. This molecule is a UVB filter known for its photo-stability. Our objective was to design UVA filters, based on the structure of a photo-stable compound. With this approach, we intended to develop UVA filters able to avoid photo-degradation, without the need of triplet-triplet quenchers.

Our approach described correctly the excitation energies of 4-MBC, thus validating our chosen methodology. Moreover, useful structure-energy relationships were uncovered. Addition of electron-withdrawing groups to C₁₅ decreases the excitation energy, and increase the oscillator strength of the new compounds. Addition of electron-donating groups to C₁₁ also leads to a red-shift, but decreases the oscillator strength. Therefore, C₁₅ appears to be the ideal localization of structure substitution. Addition of substituents to carbon atoms present in the camphor moiety do not appear to present great potential, as they are not involved in the HOMO → LUMO transition of these molecules.

More importantly, the simultaneous addition of appropriate substituents to both C₁₅ and C₁₁ resulted in the creation of two new UVA filters. The filters present red-shifts in the absorption of 0.35-0.69 eV when in comparison with 4-MBC, while the oscillator strength was still appreciably high. In conclusion, this study succeeded in the design of new UVA filters based on the photo-stable UVB filter 4-MBC. Moreover, relationships were uncovered that allow the development of more UVA filters based on 4-MBC.

Acknowledgements

A Ph.D. Grant to Luís Pinto da Silva (SFRH/BD/76612/2011), attributed by Fundação para a Ciência e Tecnologia (FCT, Portugal), is acknowledged. Margarida S. Miranda also thanks FCT for the financial support under the frame of the Ciência 2008 program.

Notes and references

^a Centro de Investigação em Química, Departamento de Química e Bioquímica, Faculdade de Ciência, Universidade do Porto, s/n, 4169-007, Porto, Portugal.

Electronic Supplementary Information (ESI) available: Cartesian coordinates of the studied molecules. Orbital representation for MBC₁₃ and MBC₁₇. See DOI: 10.1039/b000000x/

- 1 C.G. Daughton and T.A. Ternes, *Environ. Health Perspect.*, 1999, **107**, 907.
- 2 N.A. Shaath, *Photochem. Photobiol. Sci.*, 2010, **9**, 464.
- 3 P.J.O. Ferreira, L. Pinto da Silva, M.S. Miranda and J.C.G. Esteves da Silva, *Computational Chemistry: Theories, Methods and Applications*, ed. D. Bove, Nova Science Publishers, 2014, ch. 2, pp 23-42.
- 4 N.R. Attard and P. Karran, *Photochem. Photobiol. Sci.*, 2012, **11**, 62.
- 5 A. Fourtanier, D. Moyal and S. Seite, *Photochem. Photobiol. Sci.*, 2012, **11**, 81.
- 6 G.P. Pfeifer and A. Besaratinia, *Photochem. Photobiol. Sci.*, 2012, **11**, 90.
- 7 Y. Matsumura and H.N. Ananthaswamy, *Appl. Pharmacol.*, 2004, **195**, 298.
- 8 S. Mouret, A. Forestier and T. Douki, *Photochem. Photobiol. Sci.*, 2012, **11**, 155.
- 9 A.J.M. Santos, M.S. Miranda and J.C.G. Esteves da Silva, *Water Res.*, 2012, **46**, 3167.
- 10 M.S. Díaz-Cruz, M. Llorca and D. Barceló, *Trends Anal. Chem.* 2008, **27**, 873.
- 11 U. Osterwalder, and B. Herzog, *Photochem. Photobiol. Sci.*, 2010, **9**, 470.
- 12 N.A. Shaath, *The Chemistry of Ultraviolet Filters. Sunscreens*, ed. N.A. Shaath, Taylor & Francis: Boca Raton, FL, 2005, pp 217-238.
- 13 S.P. Huong, E. Rocher, J.D. Fourneron, L. Charles, V. Monnier, H. Bun and V. Andrieu, *J. Photochem. Photobiol. A*, 2008, **196**, 106.
- 14 A.J.M. Santos, M.S. Miranda and J.C.G. Esteves da Silva, *Water Res.*, 2012, **46**, 3167.
- 15 W. Schwack and T. Rudolph, *J. Photochem. Photobiol. B*, 1995, **28**, 229.
- 16 L. Pinto da Silva, P.J.O. Ferreira, D.J.R. Duarte, M.S. Miranda and J.C.G. Esteves da Silva, *J. Phys. Chem. A*, 2014, **118**, 1511.
- 17 J. Kockler, M. Oelgemoller, S. Robertson and B.D. Glass, *J. Photochem. Photobiol. C*, 2012, **13**, 91.
- 18 C.A. Bonda, *The Photostability of Organic Sunscreens Actives: a Review*, ed. N.A. Shaath, Taylor & Francis: Boca Raton, FL, 2005, pp. 321-349.
- 19 C. Paris, V. Lhiaubet-Vallet, O. Jiménez, C. Trullas and M.Á. Miranda, *Photochem. Photobiol.*, 2009, **85**, 178.
- 20 A. Kikuchi and M. Yagi, *Chem. Phys. Lett.*, 2011, **513**, 63.
- 21 S. Scalia and M. Mezzena, *Photochem. Photobiol.*, 2010, **86**, 273.
- 22 C.A. Bonda, A. Pavlovic, K. Hanson and C. Bardeen, *Cosmet. Toiletries*, 2010, **125**, 40.
- 23 C. Mendrok-Edinger, K. Smith, A. Janssen and J. Vollhardt, *Cosmet. Toiletries*, 2009, **124**, 47.
- 24 B. Herzog, M. Wehrle and K. Quass, *Photochem. Photobiol.*, 2009, **85**, 869.
- 25 E. Chatelain and B. Gabard, *Photochem. Photobiol.*, 2001, **74**, 401.
- 26 A. Kikuchi, K. Shibata, R. Kumasaka and M. Yagi, *J. Phys. Chem. A*, 2013, **117**, 1413.
- 27 D.C. Steinberg, *Regulations of Sunscreens Worldwide. Sunscreens*, ed. N.A. Shaath, Taylor & Francis: Boca Raton, FL, 2005, pp. 173-198.
- 28 H.R. Buser, M.D. Muller, M.E. Balmer, T. Poiger and I.J. Buerge, *Environ. Sci. Technol.*, 2005, **39**, 3013.
- 29 U. Hauri, B. Lutolf, U. Schlegel and C. Hohl, *Mitt. Lebensm. Hyg.*, 2004, **95**, 147.
- 30 L.R. Gasper and P.M.B.G.M. Campos, *Int. J. Pharm.*, 2006, **307**, 123.
- 31 E. Chatelain and B. Gabard, *Photochem. Photobiol.*, 2001, **74**, 401.
- 32 N. Tarras-Wahlberg, G. Stenhagen, O. Larko, A. Rosén, A.M. Wennberg and O. Wennerstrom, *J. Invest. Dermatol.*, 1999, **113**, 547.
- 33 M.J. Frisch, et al., Gaussian 09, Revision A.02, Gaussian, Inc., Wallingford CT, 2009.
- 34 C. Adamo and V. Barone, *J. Chem. Phys.*, 1999, **110**, 6158.
- 35 A. Schaefer, C. Huber and R. Ahlrichs, *J. Chem. Phys.*, 1994, **100**, 5829.
- 36 G. Scalmani, M.J. Frisch, B. Mennucci, J. Tomasi, R. Cammi and V. Barone, *J. Chem. Phys.*, 2006, **124**, 1.
- 37 F. Furche and R. Ahlrichs, *J. Chem. Phys.*, 2002, **117**, 7433.
- 38 T. Yanai, D. Tew and N. Handy, *Chem. Phys. Lett.*, 2004, **393**, 51.
- 39 L. Pinto da Silva and J.C.G. Esteves da Silva, *Int. J. Quantum Chem.*, 2013, **113**, 45.
- 40 D. Jacquemin, E.A. Perpète, I. Ciofini and C. Adamo, *Theor. Chem. Acc.*, 2011, **128**, 127.
- 41 D. Jacquemin, V. Wathelet, E.A. Perpète and C. Adamo, *J. Chem. Theor. Comput.*, 2009, **5**, 2420.
- 42 C. Adamo and D. Jacquemin, *Chem. Soc. Rev.*, 2013, **42**, 845.
- 43 M.S. Miranda, L. Pinto da Silva and J.C.G. Esteves da Silva, *J. Phys. Org. Chem.*, 2014, **27**, 47.
- 44 M. Cossi, N. Rega, G. Scalmani and V. Barone, *J. Comput. Chem.*, 2003, **24**, 669.
- 45 T. Lu and F.W. Chen, *Acta Chim. Sinica*, 2011, **69**, 2393.
- 46 T. Lu and F.W. Chen, *J. Comput. Chem.*, 2012, **33**, 580.
- 47 J. Bloino, M. Biczysko, F. Santoro and V. Barone, *J. Chem. Theory Comput.*, 2010, **6**, 1256.
- 48 F.J.A. Ferrer and F. Santoro, *Phys. Chem. Chem. Phys.*, 2012, **14**, 13549.
- 49 P. Macak, Y. Luo and H. Gren, *Chem. Phys. Lett.*, 2000, **330**, 447.